

Application of the glass-ceramic process for the fabrication of whisker reinforced celsian-composites

V. LANSMANN, M. JANSEN

Max-Planck-Institut für Festkörperforschung, Heisenbergstr. 1, D-70569 Stuttgart, Germany

E-mail: hamilton@vsibm1.mpi-stuttgart.mpg.de

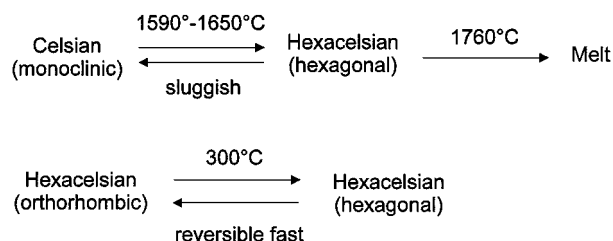
The glass-ceramic process has been investigated as an alternative route to the common ceramic process for the formation of whisker reinforced ceramic composites. In the BaSiAlTiO system composites have been prepared with celsian ($\text{BaAl}_2\text{Si}_2\text{O}_8$) as the matrix and hollandite ($\text{Ba}_{1.23}\text{Al}_{2.46}\text{Ti}_{5.54}\text{O}_{16}$) as the reinforcement. Different starting materials have been subjected to a thermal treatment, and the product samples have been studied with respect to their microstructures and the crystalline phases present. By annealing pellets of a finely powdered, quenched melt containing Ba, Si, Al and O, to which crystalline TiO_2 was added, a complete transformation of hexacelsian, formed in a first step, into celsian was achieved at 1000°C . In the celsian matrix, needle-shaped hollandite crystals precipitate, which are distributed homogeneously over the matrix phase. In these dense composites, typical reinforcement mechanisms, such as crack deflection and whisker pull-out have been observed. © 2001 Kluwer Academic Publishers

1. Introduction

A severe drawback of ceramic materials, limiting their broader application, is their brittleness, resulting in a catastrophic failure above a certain stress value. A possible remedy lies in the incorporation of fibres or whiskers in a ceramic matrix. In this way, energy-dissipating processes like debonding at the fibre-matrix interface, crack deflection, fibre pull-out, fibre bridging etc. become possible, which may improve the toughness of the ceramics [1]. Usually such ceramic composites are processed via mixing a matrix powder with a fibre component, followed by powder compaction and sintering, similar to the preparation of dense ceramics via the powder route. However, due to the addition of the second (fibre) phase specific problems arise, e.g. a decrease in densification, or clustering of the second phase [2, 3]. Depending on the length and aspect ratio of the fibres and the production process, these clusters can become rather large. These inhomogeneities, which also include not reinforced matrix zones, weaken the mechanical properties of the composite. A further essential disadvantage of using short dry fibres or whiskers is their potential for posing a health hazard, similar to that of asbestos. Considering these drawbacks of the conventional ceramic processing techniques, there is a clear need for alternative routes. A promising approach could be using a glass-ceramic process: After melting the components and quenching the melt into the glassy state, the short fibres develop in situ in the amorphous matrix during an appropriate thermal treatment. Fur-

thermore, composites produced via this process are expected to show a homogenous distribution of the fibres in the matrix, since the nucleation process for the crystal growth should start simultaneously through the whole sample [4].

For our studies of the glass-ceramic process as a possible alternative route to fibre or whisker reinforced composite ceramics, the BaSiAlTiO system seemed appropriate, both with respect to the crystalline phases present in it and their specific properties. Monoclinic celsian ($\text{BaAl}_2\text{Si}_2\text{O}_8$) is expected to form the matrix, and tetragonal barium-aluminum titanate ($\text{Ba}_{1.23}\text{Al}_{2.46}\text{Ti}_{5.54}\text{O}_{16}$), crystallizing in the hollandite type [5], should serve as the reinforcement. The hollandite phase is expected to crystallize as fibre shaped crystals because of its low c/a -ratio of 0.29 [6]. Furthermore, monoclinic celsian has a potential as a refractory ceramic and as a ceramic matrix in composites, since it exhibits a low thermal expansion coefficient ($2.3 \times 10^{-6} \text{K}^{-1}$, 20° to 1000°C) and high mechanical strength as well as oxidation-, thermal- and chemical resistance [7–10]. There are three polymorphs in the BaSiAlO system with a composition of $\text{BaAl}_2\text{Si}_2\text{O}_8$, called celsian, paracelsian and hexacelsian. Hexacelsian is a synthetic material and exists in a hexagonal and an orthorhombic modification. The properties and thermostability ranges of these phases have been discussed controversially in a number of studies. At present, the most accepted relations of the phases seem to be as follows [11, 12].



At room temperature monoclinic celsian is the thermodynamically stable form, which transforms into hexagonal hexacelsian between 1590°C and 1650°C. Hexacelsian melts at about 1760°C. On cooling, hexagonal hexacelsian rather sluggishly transforms into celsian, since breaking of Al-O- and Si-O-bonds is required in order to rearrange the atoms from the two-dimensional sheet structure of hexacelsian [13] into the three-dimensional network structure of celsian [14]. Therefore, hexagonal hexacelsian can be easily retained below the transformation temperature. At about 300°C it shows a fast reversible transformation into orthorhombic hexacelsian, which is accompanied by a decrease in volume of 3 to 4 percent. This large volume change in combination with the high thermal expansion coefficient ($8 \times 10^{-6} \text{ K}^{-1}$, 300° to 1000°C) [15] make hexacelsian unsuitable as a refractory ceramic material. Unfortunately, hexagonal hexacelsian always crystallizes first from $\text{BaAl}_2\text{Si}_2\text{O}_8$ glasses or gels. For this reason numerous attempts have been made to accelerate the slow transformation of the initially crystallized hexacelsian into celsian, e.g. by high temperature sintering, by hot isostatic pressing [16], by seeding with or by adding a variety of components [17–19]. In particular, it was found that seeding with rutile [20] in glasses or gels facilitates both the crystallization of hexacelsian and its transformation into celsian.

The general aim of our present work was to analyze the potential of the glass-ceramic process for the preparation of whisker reinforced ceramics, in principle. In more detail, we had to find out the optimal thermal treatment conditions for the system under investigation.

2. Experimental

2.1. Preparation of the melts

Mixtures (about 10 g) of reagent grade $\alpha\text{-Al}_2\text{O}_3$ (corundum), SiO_2 (amorphous), TiO_2 (anatase) and BaCO_3 with different nominal ratios of celsian to hollandite (Table I) were homogenized by ball milling and melted

TABLE I Results of the DSC measurements of the quenched melts

Sample	ratio* celsian : hollandite	endotherm. Peak T_{max} [°C]	Inflection point T_g [°C]
Ti-001	91.72:8.28	324	611
Ti-002	83.11:16.89	331	613
41	80:20	336	613
Ti-003	74.16:25.84	344	615
Ti-004	64.85:35.15	-	620
T41	80:20**	-	895

*nominal ratio referring to a complete crystallization of the raw materials into celsian ($\text{BaAl}_2\text{Si}_2\text{O}_8$) and hollandite ($\text{Ba}_{1.23}\text{Al}_{2.46}\text{Ti}_{5.54}\text{O}_{16}$).

**without TiO_2 ($\text{BaSi}_2\text{Al}_2\text{O}_8 : \text{Ba}_{1.23}\text{Al}_{2.46}\text{O}_{4.92}$, 4:1).

under constant argon flow in a high frequency furnace. A boron nitride crucible placed into a carbon crucible was used. After having kept the mixtures at 840°C for 45 min. in order to remove residual moisture, they were heated up to about 1850°C, a temperature at which a homogenous melt formed. The melt was kept for 20 min. at this temperature and subsequently quenched to room temperature by switching off the furnace and guiding a strong flow of argon through the heating zone. The average cooling rate was about 10–15 K/s from the maximum temperature to about 800°C.

Sample T41 (Table I) corresponds to sample 41 except that at first instead of a BaSiAlTiO melt a BaSiAlO melt was prepared. The TiO_2 required to adjust the celsian to hollandite ratio of 4 : 1 was added before the following sintering step.

2.2. Preparation of the composite ceramics

The thermal treatment of composites were focused on samples with an overall composition corresponding to a nominal celsian to hollandite ratio of 4 to 1. The following four types of starting materials have been used:

1. Bulk pieces of the quenched BaSiAlTiO melt
2. Pellets of the powdered quenched BaSiAlTiO melt
3. Pellets of the quenched BaSiAlO melt to which TiO_2 (anatase) was added before homogenizing and compacting in order to adjust the desired celsian to hollandite ratio
4. Pellets of the mixed raw materials BaCO_3 , $\alpha\text{-Al}_2\text{O}_3$ (corundum), TiO_2 (anatase), and SiO_2 (amorphous).

The pellets were prepared by pressing the powders unidirectionally (at about 460 bar) after ball milling of the mixtures of the starting materials and/or crunched melts.

All samples were subjected to the thermal treatment under identical conditions in a silicon carbide furnace in air within an alumina crucible. The heating rate up to the maximum temperature (800°C to 1400°C) was 100°C/h. The maximum temperature was varied in 100°C steps, and the samples were kept for 24 hours at that temperature before cooling to room temperature with a cooling rate of 100°C/h.

2.3. Analytical procedures

The X-ray diffractometer used was a Stadi P (Stoe&Cie GmbH) with $\text{Cu-K}\alpha_1$ radiation. The crystalline phases were identified by referring to the powder diffraction file (PDF) prepared by international centre for diffraction data or by using single crystal structure data from the inorganic crystal structure database (ICSD) for simulating powder diffraction diagrams. The thermal behavior of the quenched melts was investigated using a DSC 404 (Netzsch, argon atmosphere, heating rate 10°C/min.), calibration by Al_2O_3 discs. The scanning electron microscope DSM 940 (Zeiss) equipped with the EDX setup EDAX PV9800 was used for the analysis of the microstructure and the local elemental composition.

3. Results and discussion

The powder diffraction diagrams of all quenched BaSiAlTiO melts (Fig. 1) indicate that hexacelsian is the only crystalline phase, besides amorphous material. Consequently, titanium must be part of the residual glassy network. The powder diffraction diagram of the BaSiAlO melt (T41 in Fig. 1) reveals that only a very small amount of hexacelsian has crystallized during quenching, and that mainly an amorphous phase has formed.

The DSC scans of the quenched BaSiAlTiO melts are similar to each other (Fig. 2, Table I). The melts with hollandite between 8 and 26% show an endothermic peak with a maximum at approximately 320°C, which might correspond to the hexacelsian transition of the orthorhombic to the hexagonal modification. The peak maximum is shifted to a higher temperature, and the intensity of the peak weakens with a growing share of

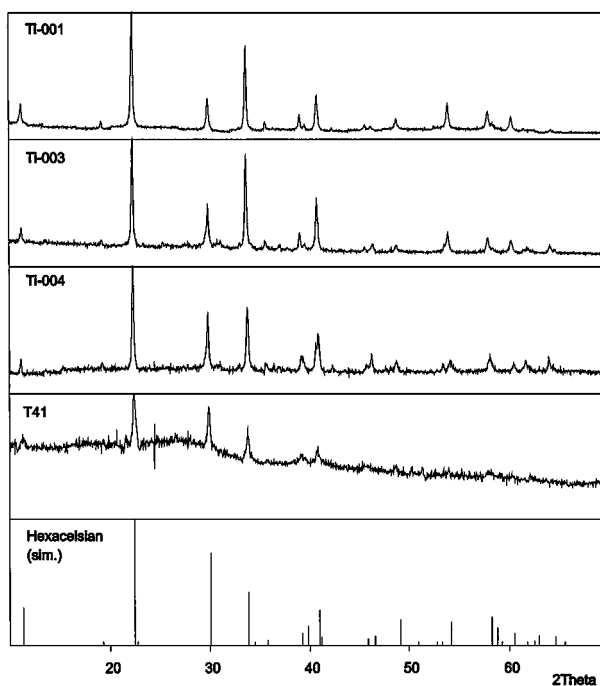


Figure 1 X-ray powder diffraction diagrams of the quenched melts Ti-001, Ti-003, Ti-004 and T41 as well as the peak diagram of hexacelsian simulated by means of single crystal structure data from ICSD 38215.

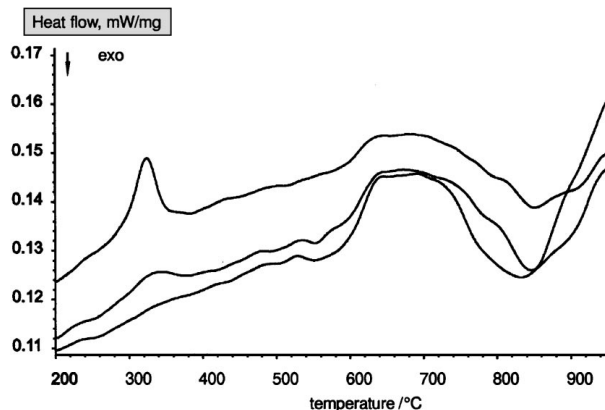


Figure 2 DSC curves of quenched BaSiAlTiO-melts Ti-001, Ti-003 and Ti-004 using a scan rate 10°C/min. (argon atmosphere).

hollandite in the starting mixture. Finally, in the sample Ti-004 the content of hexacelsian is too low for the transition of hexacelsian to be recorded using DSC. All quenched BaSiAlTiO melts show a glass transition above 610°C, which shifts slightly to a higher temperature with increasing content of hollandite. At about 840°C all samples show a broad exothermic peak, which seems to be related to further crystallization of hexacelsian, this being the only crystalline phase identified by X-ray diffraction in the samples after the DSC scan (Fig. 4). When comparing the melt 41 with the corresponding titanium free BaSiAlO-melt T41, an increase of the glass transition temperature by almost 300°C is found, obviously due to omitting TiO₂ (Fig. 3). This glass transition temperature for the BaSiAlO-glass is in accordance with results found by other authors e.g. [21]. This clearly points to the fact that titanium lowers the viscosity of the glass and therefore the glass transition temperature. The X-ray diffraction diagram of the BaSiAlO melt after the DSC measurement (Fig. 4) can serve as reference for a further crystallization of hexacelsian during the heating process (high amount of glassy phase remained in this sample as compared to the corresponding BaSiAlTiO sample).

The results of the phase analysis after the thermal treatment of the different starting materials with a

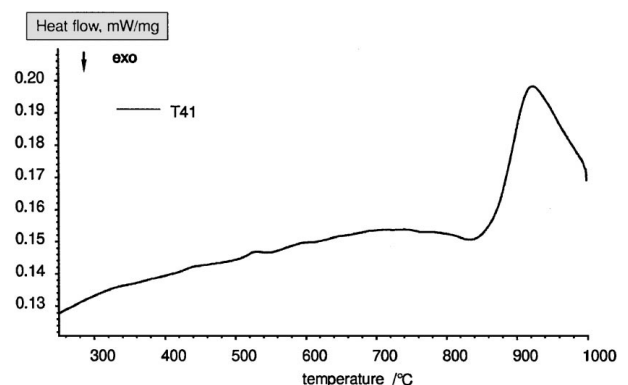


Figure 3 DSC curve of the quenched BaSiAlO-melt T41 using a scan rate of 10°C/min. (argon atmosphere).

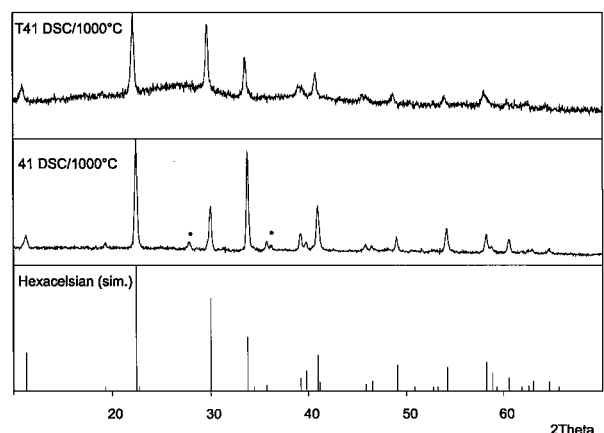


Figure 4 X-ray powder diffraction diagrams of the quenched BaSiAlTiO-melt 41 and the quenched BaSiAlO-melt T41 after the DSC run up to 1000°C using a scanning rate of 10°C/min. as well as the simulated peak diagram of hexacelsian. The stars denote two additional peaks, which are too weak to be unambiguously assigned to a certain crystalline phase.

TABLE II Crystalline phases in the powder diffraction diagrams of the different starting materials after thermal treatment identified by comparison with the peak diagrams of the PDF or with the corresponding diagrams simulated by means of the ICSD

sample	T_{\max} [°C]						
	800	900	1000	1100	1200	1300	1400
Fragments	H(v.st.)	H(v.st.)	H(v.st.)	H(v.st.)	H(v.st.)	C(v.st.)	H(v.st.)
BaSiAlTiO-			Hol(w.)	Hol(w.)	C(st.)	H(st.)	Hol(w.-m.)
melt				Ru(v.w.)	Hol(m.)	Hol(m.)	Cel(w.-m.)
pellets of	H(v.st.)	H(v.st.)	H(v.st.)	H(v.st.)	C(v.st.)	C(v.st.)	C(v.st.)
powdered	An(w.)	Ru(w.)	Hol.(w.-m.)	Ru(w.-m.)	Hol(m.)	Hol(m.)	Hol(m.)
BaSiAlTiO-	Ru(v.w.)	Hol(v.w.)	C(w.)	Hol(w.)			
melt			Ru(v.w.)				
pellets of	H(v.st.)	H(v.st.)	C(v.st.)	C(v.st.)	C(v.st.)	C(v.st.)	C(v.st.)
BaSiAlO-	An(v.st.)	Ru(w.-m.)	Hol(m.)	Hol(m.)	Hol(m.)	Hol(m.)	Hol(m.)
melt/mixed		An(w.)					
with TiO ₂							
pellets of	BT(v.st.)	BT(v.st.)	BT(v.st.)	H(v.st.)	C(v.st.)	C(v.st.)	C(v.st.)
the raw	BS(m.)	K(w.-m.)	BA(m.)	Fr(m.)	Hol(m.)	Hol(m.)	Hol(m.)
materials	An(m.)	BA(w.-m.)	H(m)	BA(m)			
BaCO ₃ ,	K(m.)	BS(v.w.)	Fr(m.)	BT(m.)			
Al ₂ O ₃ ,	BA(m.)		Q(w.-m)	Q(m)			
SiO ₂ , TiO ₂			K(w.)	C(w.-m.)			

Intensities: v.st. very strong, st. strong, m. medium, w. weak, v.w. very weak.

Crystalline phases: C celsian BaAl₂Si₂O₈ (PDF 38-1450), H hexacelsian BaAl₂Si₂O₈ (ICSD 38215), Hol hollandite Ba_{1,23}Al_{2,46}Ti_{5,54}O₁₆ (PDF 33-133), An anatase TiO₂ (PDF 21-1272), Ru rutile TiO₂ (PDF 21-1276), BA barium aluminate BaAl₂O₄ (PDF 17-306), BS barium silicate Ba₂SiO₄ (PDF 26-1403), BT barium titanate BaTiO₃ (PDF 5-626), K corundum α -Al₂O₃ (PDF 10-173), Q quartz α -SiO₂ (PDF 33-1161), Fr fresnoite Ba₂TiSi₂O₈ (PDF 18-197).

nominal celsian/hollandite ratio of 4 : 1 as a function of the maximum annealing temperature are summarized in Table II.

In the annealed quenched BaSiAlTiO melt, the crystallization of hollandite starts at 1000°C. However, the transformation of hexacelsian into celsian required at least 1200°C, and was not complete even at 1300°C. As already mentioned in the introduction it is well known that the transformation of hexacelsian into the thermodynamic more stable celsian is a sluggish process and many attempts were made to speed it up [10, 13–20]. Comparing these results with the development of the

crystalline phases in this temperature range, the formation of large amount of hexacelsian at the expense of celsian at 1400°C is surprising, because (crystalline bulk) celsian is the thermodynamic stable phase until 1590°C. Thus the approach to prepare a composite consisting of celsian and hollandite only by applying the common glass-ceramic process of quenching a melt followed by a thermal treatment of the bulk glassy solid was not successful.

Considering our observation and former results of other others [22] that the transformation of hexacelsian into celsian starts at the surface, we milled and

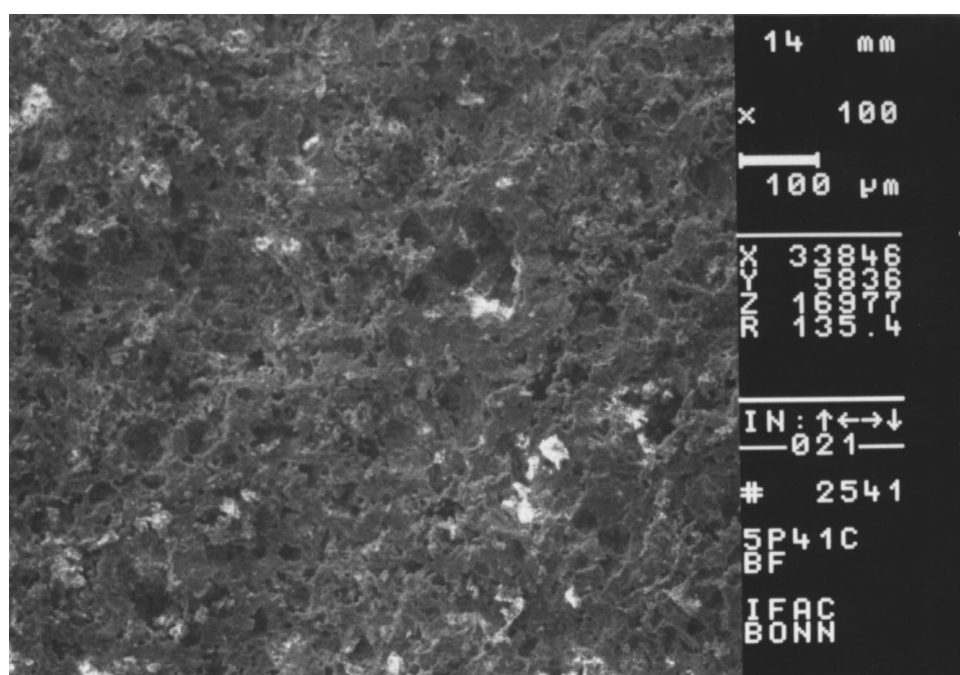


Figure 5 SEM micrographs of the pellets of the raw materials after annealing at 1200°C for 24 h.

pressed the BaSiAlTiO glass before annealing in order to speed up this transformation by increasing the surface. In such samples hexacelsian had transformed completely into celsian at 1200°C, and the crystalline phases of the desired composite had formed. Hollandite and celsian remain stable until 1400°C. Another significant difference to the results on bulky glass samples lies in the fact that at 800°C TiO₂ (anatase and rutile) had crystallized. Obviously, in a first step TiO₂ precipitates from the glass, and in a second step, the hollandite phase crystallizes. Therefore, to facilitate the crystallization of hollandite by skipping the step of TiO₂ separation, anatase was added to pure BaSiAlO glass before powdering, compacting and annealing. Using

BaSiAlO instead of BaSiAlTiO glass, an increase of the glass-transition temperature is to be expected due to the viscosity decreasing effect of TiO₂ in silicate glasses. During this altered procedure celsian and hollandite formed as the only crystalline phases at temperatures above 1000°C.

Thus, the transformation of hexacelsian into celsian was complete at 200°C below that needed in any other approach. Two main effects seem to contribute to this different crystallization behavior. Firstly, the glass-transition temperature of the BaSiAlO melt is about 300°C higher resulting in a much lower content of hexacelsian, which later has to be transformed into celsian, in the quenched melt. Secondly, in accordance with the

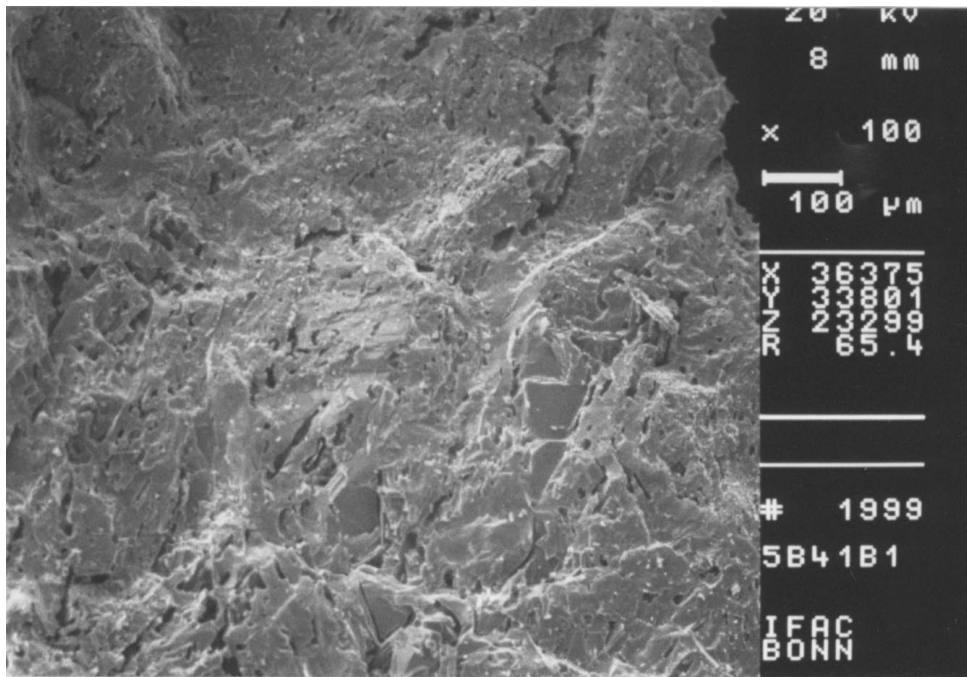


Figure 6 SEM micrographs of the bulk quenched BaSiAlTiO-melt after annealing at 1200°C for 24 h.

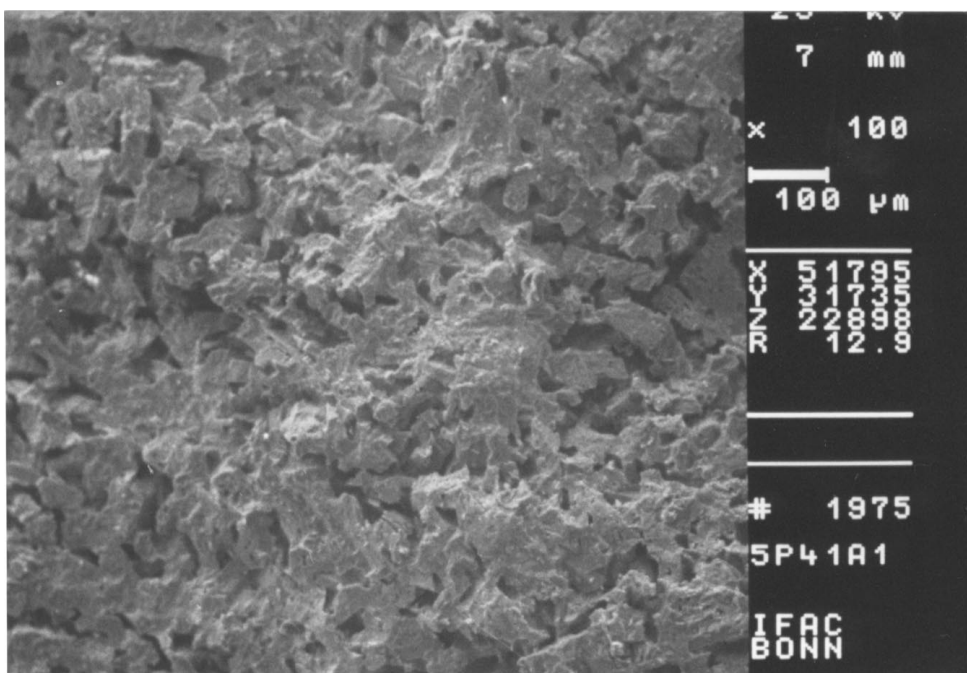


Figure 7 SEM micrographs of the pellet of powdered BaSiAlTiO-melt after annealing at 1200°C for 24 h.

investigations of Liu *et al.* [20], the presence of crystalline TiO_2 at the beginning of the crystallization process of the glassy phase speeds up the nucleation of both hexacelsian and celsian. With respect to the objectives of our work, this latter approach is superior to all alternatives tried, and yields the desired composite of celsian and hollandite at 1200°C .

Figs 5 to 9 give an overview of the microstructures of the samples, prepared via different routes, and thermally treated at 1200°C for 24 h. Noticeable are the differences in the porosity of the samples. The composite of the pressed and annealed raw materials (Fig. 5) exhibits the highest porosity. In contrast, the tempered

bulk BaSiAlTiO glass shows a low crystallinity (Fig. 6). Long cracks ($>100\ \mu\text{m}$) and holes are running straight through dense melt-like areas of the ceramic. The compacted powder of the quenched BaSiAlTiO melt reveals a more homogenous distribution of pores (Fig. 7) which, in addition, are smaller, about few tenths of a micron in diameter. Needle-shaped hollandite crystals are embedded in a melt-like matrix of celsian. The porosity and the aspect ratio of the hollandite crystals can be influenced by the thermal treatment. After annealing for 24 h at 1400°C , the composite exhibits a more crystalline and dense microstructure, although a quite high residual porosity (Fig. 10) is still present. The SEM

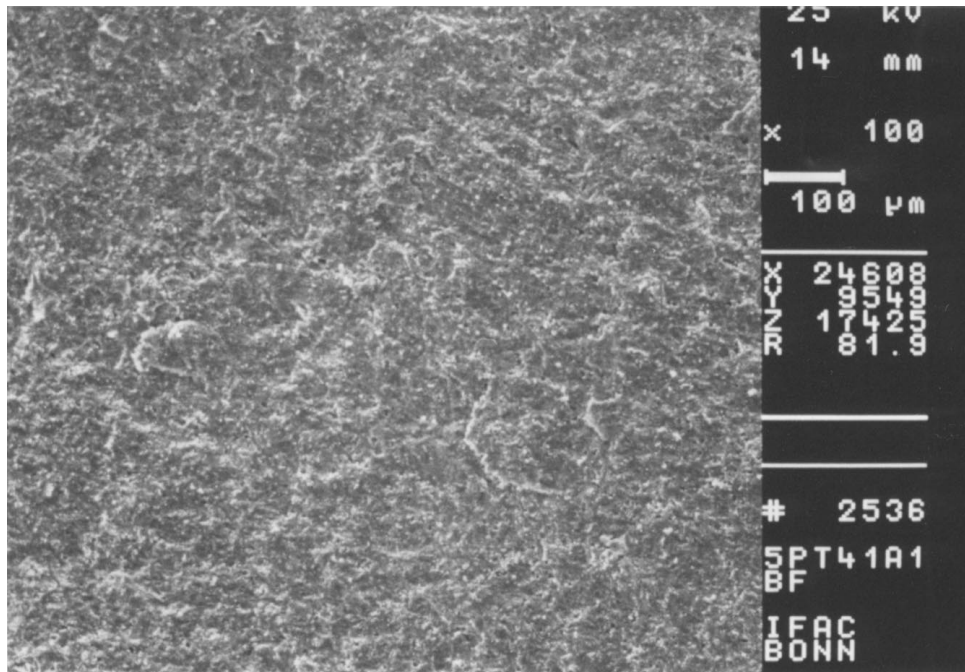


Figure 8 SEM micrographs of the pellet of powdered BaSiAlO -melt mixed with TiO_2 after annealing at 1200°C for 24 h.

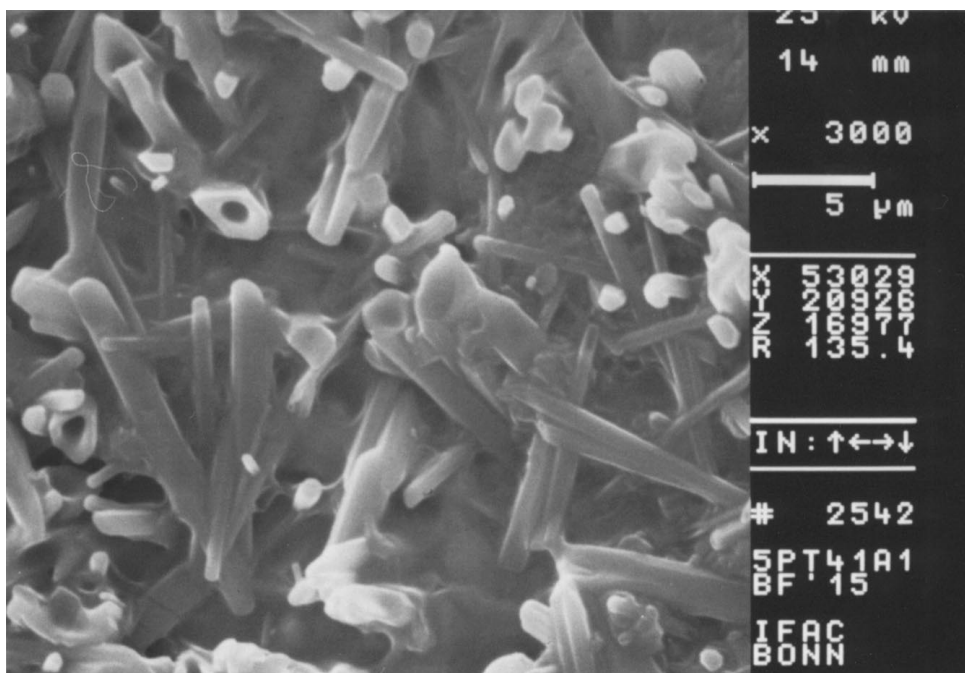


Figure 9 SEM micrographs of the fracture surface of the pellet of powdered BaSiAlO -melt mixed with TiO_2 after annealing at 1200°C for 24 h and thermally etching for 15 min. at 1200°C .

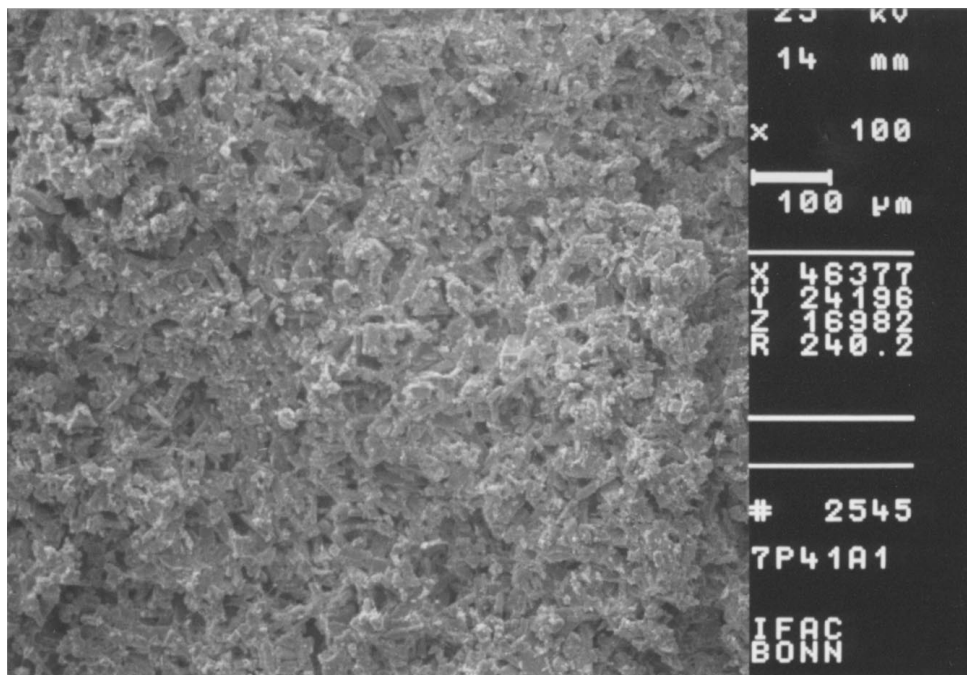


Figure 10 SEM micrographs of the pellet of powdered BaSiAlTiO-melt after annealing at 1400°C for 24 h.

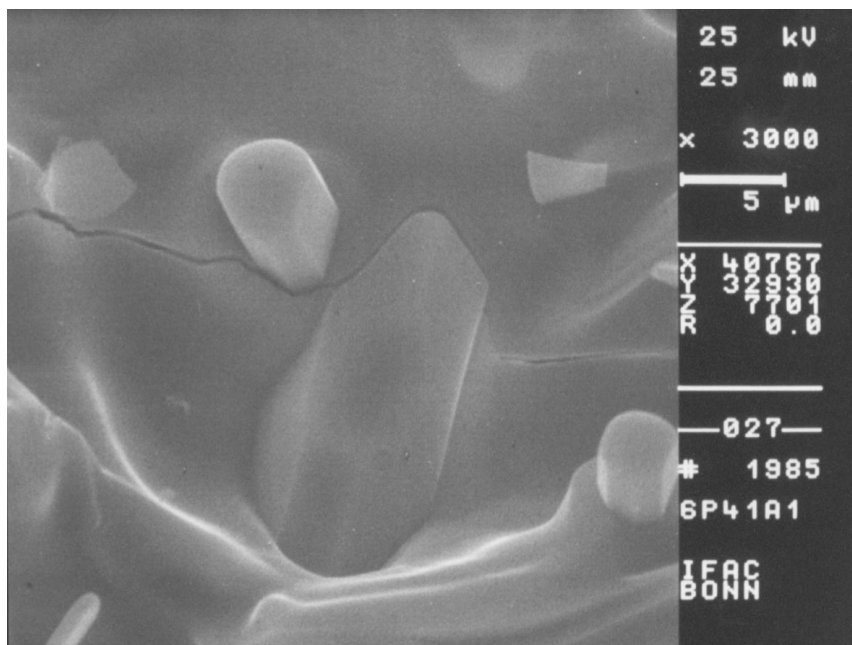


Figure 11 SEM micrograph of the pellet of powdered BaSiAlTiO-melt after annealing at 1300°C for 24 h.

micrographs further demonstrate that a higher annealing temperature increases the aspect ratio of the hollandite crystals.

In contrast to the composites based on BaSiAlTiO melts, the annealed compacted BaSiAlO glassy powders mixed with TiO₂ have a high density (Fig. 8). The ceramic shows only few pores with less than ten microns in diameter. After an additional thermal treatment for 15 min. at 1200°C, the fractured surface of the composite shows a homogenous distribution of needle-shaped hollandite in a celsian matrix (Fig. 9).

Fig. 11 shows a crack track through a sample obtained by annealing powdered BaSiAlTiO glass. The crack running from left to right is first deflected by a hollandite crystal, at another position a hollandite crys-

tal is pulled out of the matrix. So both typical reinforcement mechanisms - crack deflection and whisker pull-out - can be observed in the composite.

4. Conclusions

Our results in the BaSiAlTiO system demonstrate that the glass-ceramic process is in principle suited for the preparation of fibre penetrated composites, and could serve as a novel alternative approach to the common route to whisker reinforced ceramics. It provides the advantages that handling dry whiskers is avoided by crystallizing the whisker component in situ and that a homogenous distribution of the whiskers in a ceramic matrix can be achieved. In more detail, in the

investigated BaSiAlTiO system composites were obtained with celsian ($\text{BaAl}_2\text{Si}_2\text{O}_8$) as the matrix material and needle-shaped barium-aluminum titanate ($\text{Ba}_{1.23}\text{Al}_{2.46}\text{Ti}_{5.54}\text{O}_{16}$) as the reinforcement. The latter crystallize in situ during the annealing process and are distributed homogeneously in the composite. The crystalline phases present and the microstructure of the final composite strongly depend on the starting conditions and the thermal treatment. A modified glass-ceramic process, with adding TiO_2 to a quenched BaSiAlO melt before powdering and compacting, leads to a dense composite of hollandite and celsian. During annealing, hexacelsian transforms completely into celsian at 1000°C , i.e. about 150 to 200°C lower than reported until now under otherwise similar conditions. Finally, the investigations of crack tracks shows that crack deflection and whisker pull-out are present, demonstrating the desired improvements in the brittleness of the composite.

Acknowledgement

The authors gratefully acknowledge the financial support by the Deutsche Forschungsgemeinschaft (DFG), Bonn (Germany), especially within the Sonderforschungsbereich 408.

References

1. K. CHAWLA, "Ceramic Matrix Composite" (Chapman & Hall, London, 1993).
2. T. N. TIEGS and P. F. BECHER, *Amer. Ceram. Soc. Bull.* **66** (1987) 339.

3. J. V. MILEWSKI, *Adv. Ceram. Mater.* **1** (1986) 36.
4. Z. STRNAD, "Glass Ceramic Materials" (Elsevier, Amsterdam, 1986).
5. M. WATANABE, Y. FUJIKI, Y. KANAZAWA and K. TSUKIMURA, *J. Solid State Chem.* **66** (1987) 56.
6. Natl. Bur. Stand. (U.S.) Monogr. **25**(18) (1981) 10.
7. A. NORDMANN, Y.-B. CHENG and B. C. MUDDLE, *J. Europ. Ceram. Soc* **15** (1995) 787.
8. A. BANDYOPADHYAY, P. B. ASWATH, W. D. PORTER and O. B. CAVIN, *J. Mater. Res.* **10** (1995) 1256.
9. W. ZHOU, L. ZHANG and J. YANG, *J. Mater. Sci.* **32** (1997) 4836.
10. I. G. TALMY, D. A. HAUGHT, J. A. ZAYKOSKI and E. J. WUCHINA, *Ceram. Trans.* **52** (1995) 105.
11. H. C. LIN and W. R. FOSTER, *Amer. Mineral.* **53** (1968) 134.
12. J. S. M. CORRAL and A. G. VERDUCH, *Trans. J. Br. Ceram. Soc.* **77** (1978) 40.
13. B. YOSHIKI and K. MATSUMOTO, *J. Amer. Ceram. Soc.* **34** (1951) 283.
14. N. P. BANSAL and C. H. DRUMMOND III, *J. Mater. Sci. Lett.* **13** (1994) 423.
15. Y. TAKEUCHI, *Min. J. Japan* **2**(5) (1958) 311.
16. C. H. DRUMMOND and N. P. BANSAL, *Ceram. Eng. Sci. Proc.* **11**(7/8) (1990) 1072.
17. D. BAHAT, *J. Mater. Sci.* **4** (1969) 847.
18. C. H. DRUMMOND III, W. E. LEE, N. P. BANSAL and M. J. HYATT, *Ceram. Eng. Sci. Proc.* **10** (1989) 1485.
19. C. H. LIU, S. KOMARNENI and R. ROY, *J. Amer. Ceram. Soc.* **78** (1995) 2521.
20. C. LIU, S. KOMARNENI and R. ROY, *Mat. Res. Soc. Symp. Proc.* **346** (1994) 721.
21. M. J. HYATT and N. P. BANSAL, *J. Mater. Sci.* **31** (1996) 172.
22. N. P. BANSAL and C. H. DRUMMOND, *J. Amer. Ceram. Soc.* **76** (1993) 1321.

Received 6 May 1999

and accepted 26 September 2000